

Browser-based Hyperbolic Visualization

Stephen Kobourov and Jacob Miller

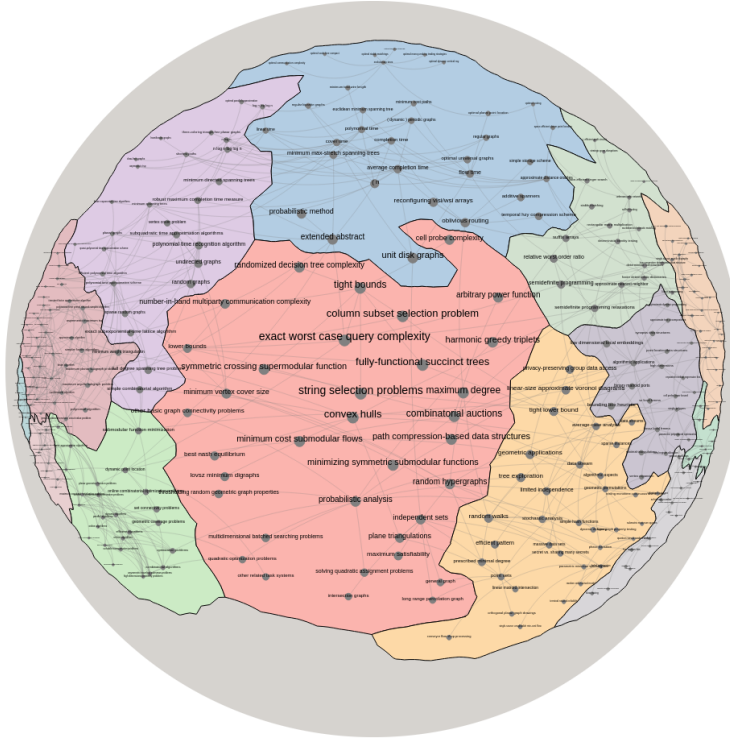
Department of Computer Science, University of Arizona

Abstract. While most graphs are drawn in the 2-dimensional Euclidean plane, some properties of non-Euclidean geometries may be beneficial for graph visualization. Some graphs can be better embedded in hyperbolic space than in Euclidean space and hyperbolic geometry provides natural “focus+context,” with parts of the graph near the center of the view shown large and those far from the center progressively smaller. We consider two methods for hyperbolic visualization of graphs in the browser. The first makes use of hyperbolic analogues to spherical projections. We integrate it with the GMap system to provide GMaps, MapSets, BubbleSets, and LineSets, as well as traditional node-link diagrams. The second method relies on a generalization of force-directed algorithms to non-Euclidean geometries, making better use of the underlying geometry.

1 Introduction

Node-link representations of graphs in the 2-dimensional Euclidean plane are the most typically used graphs visualizations. The structure of many graphs, notably planar graphs, can be realized well in the plane, but others are better represented in non-Euclidean geometries. For example, 3-dimensional polytopes are well represented in spherical space, while large hierarchies such as trees can be cleanly embedded in hyperbolic space. Standard hyperbolic projections into Euclidean space also provide a natural “focus+context” view of the graph, with parts of the graph near the center of the view shown large and those far from the center progressively smaller. There is also some evidence that hyperbolic geometry often underlies complex networks [21]. Though there has been some work on visualizing hierarchies using hyperbolic space in the browser [14], there are no tools that support browser-based hyperbolic visualization of general graphs.

We describe two methods to laying out graphs in the 2-dimensional hyperbolic space, H^2 . The first method relies on taking a pre-computed Euclidean layout of a graph and projecting it into hyperbolic space, providing standard map interactions, such as pan, zoom, re-center, click and drag. We implement this method in GMap, a graph visualization system that provides several layout algorithms for node-link and map-based visualization. This allows us to view and interact with GMaps, MapSets, BubbleSets, and LineSets in hyperbolic space. The second method makes use of a generalization of force-directed algorithms to Riemannian geometries [20]. We exploit the locally Euclidean properties of hyperbolic space so that together with Möbius transformations we can accurately



13 **Fig. 1.** Hyperbolic realization of the SODA graph described in Appendix A using
 14 a GMap style visualization.

38 model the forces. In particular, this approach allows us to compute layouts where
 39 distances between nodes in hyperbolic space correspond to the underlying graph-
 40 theoretic distances between them.

41 2 Related Work

42 The graph layout problem typically involves placing nodes and routing edges in
 43 2-dimensional Euclidean space. Force-directed algorithms model the system as a
 44 set of springs and attempt to balance the forces on nodes. Both their conceptual
 45 simplicity and their generally aesthetically pleasing results have made this class
 46 of algorithms particularly useful for computing graph layouts [19]. Force-directed
 47 algorithms have been generalized to Riemannian geometries, (e.g., spherical and
 48 hyperbolic) by computing tangent planes at each node [20].

49 To the best of our knowledge, there are no browser-based tools for visualizing
 50 general graphs in hyperbolic space. One of the earliest approaches by Lamping *et*
 51 *al.* [23] embeds hierarchies into the hyperbolic plane by recursively placing each
 52 node's children evenly spaced around the arc of a circle. This is possible thanks

to the exponential expansion intrinsic to the geometry. They make use of the Poincaré projection to display the graph on the computer monitor, which also provides the now well known “focus+context” effect. Navigating the hierarchy is done by re-centering the projection at a new point in the hyperbolic plane. The embedding can be computed in linear time and arbitrary graphs can also be visualized using this approach by utilizing a spanning tree of the graph and “filling in” the rest of the edges later.

A bioinformatics-motivated java application by Bingham and Sudarsanam [6] uses a similar approach to visualize phylogenetic trees. Andrews *et al.* [2] also rely on Lamping *et al.*’s work in their Hierarchy Visualization System as do Baumgartner and Waugh [4] who visualize Roget’s thesaurus. The Java InfoVis Toolkit also implements a hyperbolic hierarchy browser [5] and TreeBolic implements the hyperbolic tree layout [8]. More recently, Glatzhofer developed a hyperbolic hierarchy browser utilizing d3.js, a javascript graphics library which works in the browser, and can display large hierarchies smoothly with several different layout algorithms [13,14,15].

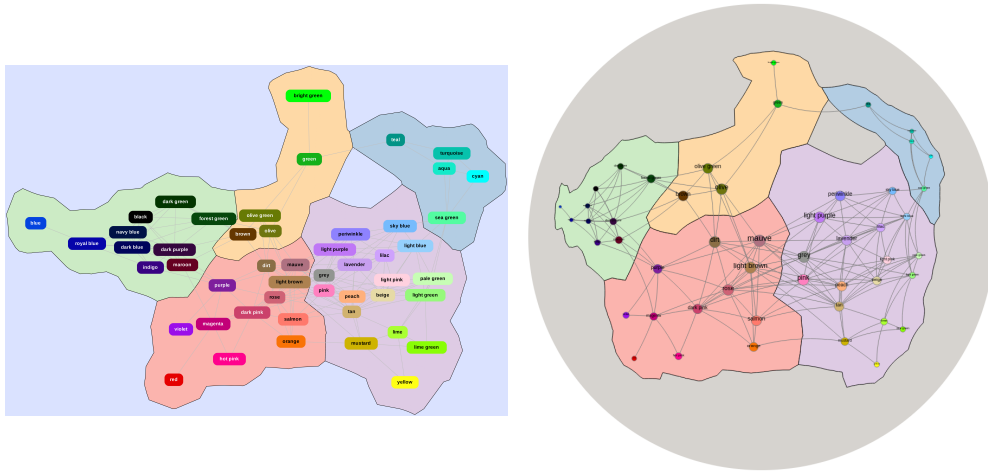
While most prior work considers the 2-dimensional hyperbolic plane, Munzner has also used 3D hyperbolic space to visualize hierarchies with the help of the Beltrami-Klein projection [26,27,28,29]. Here geodesics are mapped to straight lines rather than the circular arcs of the Poincaré projection. Munzner’s work has been re-implemented in two subsequent systems: Walrus [17] and h3py [39].

Hyperbolic space has been explored in the context of dimensionality reduction, specifically multi-dimensional scaling (MDS). This technique attempts to closely match pairwise similarities with distances in an embedding; the more similar two elements are, the closer they are in the embedding. The Euclidean distance is traditionally used as a closeness metric but Walter and Ritter describe a method that replaces the Euclidean distance metric with hyperbolic distance [38]. Computing a graph layout can be interpreted as an MDS problem by treating the graph theoretic distance between pairs of nodes as their pairwise similarity metric. It has been shown that some graphs can achieve lower distortion with fewer dimensions in hyperbolic space than in Euclidean space [7].

Recently, an open-source hyperbolic visualization tool RogueViz includes many projections and educational tools, although its restriction to tessellations of the hyperbolic plane make it less than ideal for graph drawing [9]. Self-organizing maps have been generalized to hyperbolic space, but are restricted to lattices [31].

3 Projection-based Method

The first method we present is based on the idea of starting with a precomputed layout and projecting it to the hyperbolic plane. The implementation is available at <http://gmap.cs.arizona.edu> under “advanced options.” GMap is a browser based graph visualization system that offers several layout algorithms, clustering algorithms and visualization styles, focused on map-like representations [12]. In addition to node-link diagrams, GMap provides different style visualizations, in-



89 **Fig. 2.** On the left, a Euclidean map of a GMap graph. On the right, its Hyper-
 90 bolic inverse projection.

98 cluding MapSets [11], BubbleSets [10], and LineSets [1]. Several human-subject
 99 studies suggest that such map-like visualizations are at least as good as tradi-
 100 tional node-link diagrams when it comes to task performance, memorization,
 101 and recall of the data [33,34].

102 GMap layouts are saved in the graphviz DOT file format which includes
 103 graph-wide attributes, a node list, and an adjacency list. Additionally, each node
 104 and edge have a set of attributes. GMap computes the layout and stores their
 105 position as Cartesian coordinates. This is sufficient to draw node-link diagrams
 106 and the other map-like layouts: GMaps, MapSets, BubbleSets and LineSets. For
 107 these, polygons given as a set of vertices are stored as a graph-wide attribute
 108 along with colors. The parsing of these polygons is achieved using the same
 109 implementation as Perry *et al.* [32].

111 GMap relies on two different layout algorithms for computing a Euclidean
 112 layout: *sdfp* is a multi-level force-directed algorithm [16] and *neato* is a imple-
 113 mentation of the Kamada-Kawai algorithm [18]. Figure 4 shows an example of
 114 the *colors graph* drawn as a node-link and GMap diagram. This is a graph of the
 115 38 most popular RGB colors, courtesy of xkcd¹. Figure 3 shows the same graph
 116 using the BubbleSets and LineSets options.

117 We make use of a javascript library called Hyperbolic Canvas [3]. It is a
 118 mathematical model of the Poincaré disk projection of hyperbolic space that
 119 allows lines and shapes to be drawn using an HTML canvas. The projection-
 120 based pipeline below is based on the approach by Perry *et al.* for browser-based
 121 visualization of graphs on the sphere [32].

110 ¹ <https://xkcd.com/color/rgb/>

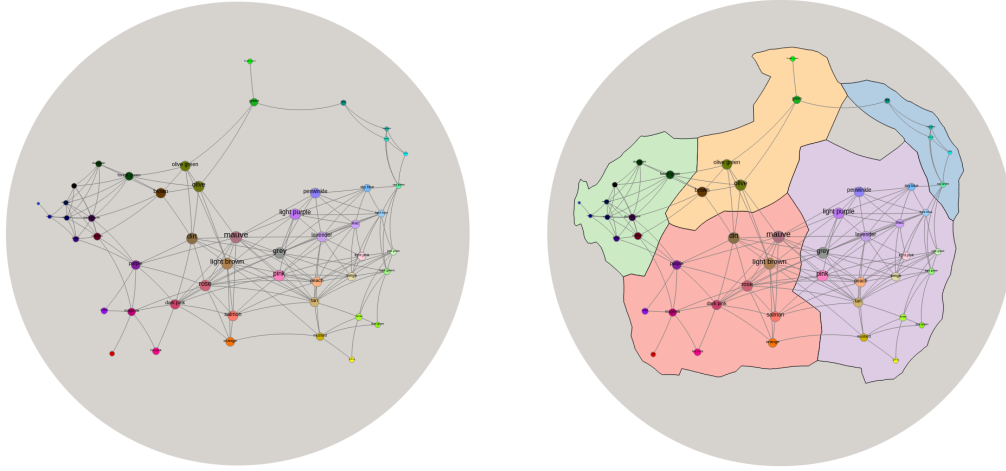


Fig. 3. A node-link and GMap diagram of the colors graph.

3.1 The Projection-based Pipeline

Given a pre-computed 2-dimensional Euclidean layout, the projection-based method can be summarized as follows:

1. Calculate geometric mean of the 2-d Euclidean layout
2. Apply an inverse hyperbolic Lambert azimuthal projection centered on the geometric mean
3. Project back into the Euclidean plane of the browser using the Poincaré projection (providing the look and feel of hyperbolic space).

Hyperbolic projections: It is well known that non-Euclidean spaces (such as spherical and hyperbolic spaces) can not be perfectly projected to the Euclidean plane. No matter what type of projection is used, something will get lost in the translation: distances are distorted, or region areas are distorted, or angles are distorted. This problem is well studied in cartography in the context of projecting the sphere onto the 2-d Euclidean plane.

Knowing that a perfect embedding in the plane is impossible, useful maps can still be created by choosing which information to preserve. Three well-known projections of the sphere are gnomonic, orthographic, and stereographic projections. The gnomonic projection preserves straight lines; geodesics of the sphere are shown as straight lines in the projection. This is particularly useful in flight planning, and is said to be the oldest map projection. The orthographic projection resembles the view of the Earth from space, and preserves scale at the center of the projection, making it useful in visualization. Finally, the stereographic projection preserves angles and has its roots in star charts used in sailing [37]. Of course, many more spherical projections exist, inspiring this xkcd comic.²

² <https://xkcd.com/977/>

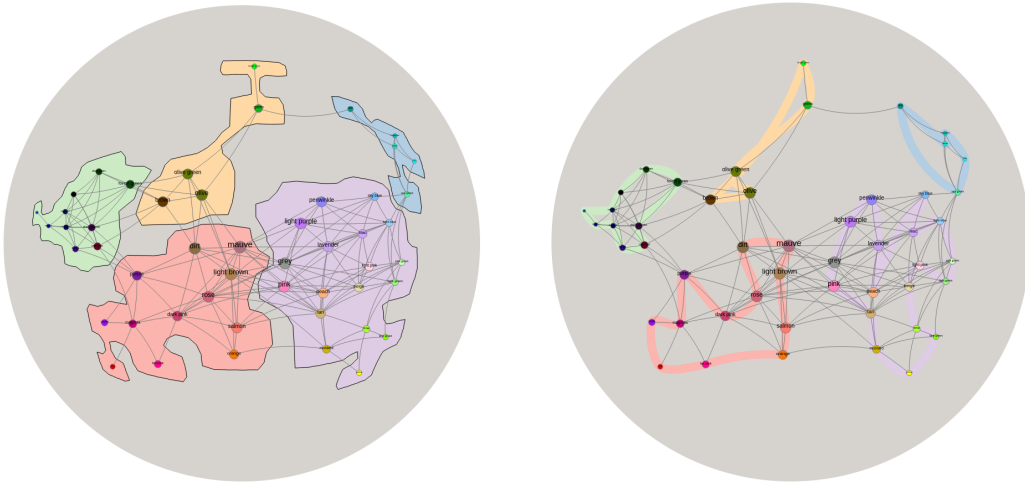


Fig. 4. BubbleSets and LineSets visualizations of the colors graph.

Hyperbolic surface is curved (negatively) just like spherical space is curved (positively), resulting in similar problems when attempting to display it in the plane of a monitor or on a piece of paper. Just as the sphere has many projections that serve different purposes, so there exists many hyperbolic projections to the plane, although they are not as well studied. These projections can be thought of as analogous to their spherical counterparts. Not only do they preserve the same information but they can often be derived in an analogous way. For instance, the Beltrami-Klein projection is analogous to the gnomonic projection of the sphere; they both preserve geodesics as straight lines. Similarly, the Gans model of the hyperbolic plane is analogous to the orthographic projection, in that they both have a point of perspective at infinity. The Poincaré projection is a spherical analogue of the stereographic projection as they both preserve angles.

Hyperbolic Lambert azimuthal projection Since we know we are projecting node-link and map diagrams, it seems reasonable to choose to preserve areas. One way this can be accomplished is through a less common hyperbolic analogue to the Lambert azimuthal projection, which has been called the hyperbolic Lambert azimuthal projection. This projection is equi-areal, so area is preserved. The hyperbolic analogue can be derived in much the same way as the sphere.

Consider two discs: one in the 2-dimensional Euclidean space and the other in the 2-dimensional hyperbolic space. Denote the area of the Euclidean disk of radius r as $e(r)$ and the area of a hyperbolic disk of the same radius $h(r)$. We want a function $f(r)$ such that $e(r) = h(f(r))$. Assuming unit curvature, then

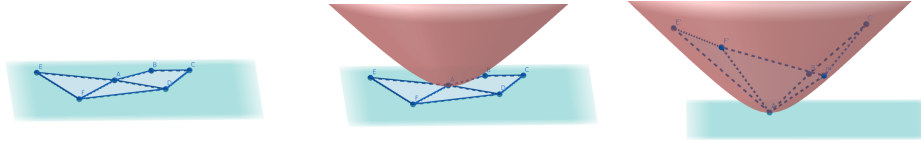
$$h(r) = 2\pi(\cosh(r) - 1)$$

$$e(r) = \pi r^2$$

174 Then substitution reveals

$$175 \quad f(r) = \operatorname{arccosh}\left(\frac{1}{2}r^2 + 1\right),$$

176 where *arccosh* is the inverse hyperbolic cosine. Note that this is the inverse
 177 projection as we go from the Euclidean plane to the hyperbolic plane. This gives
 178 us the transformation $(r, \theta) \rightarrow (f(r), \theta)$, which preserves areas, but distorts
 179 angles and shapes. The further away a shape is from the projection center the
 180 greater the distortion, so centering about the geometric mean reduces this effect.



181 **Fig. 5.** An illustration of the inverse hyperbolic Lambert azimuthal projection
 182 from the 2-d plane to the surface of a hyperboloid.

183 **Poincaré projection** Recall that the Poincaré projection of the hyperbolic
 184 plane is similar to the stereographic projection of the sphere, in that it preserves
 185 angles. The infinite hyperbolic plane is mapped to the inside of the unit disk
 186 with hyperbolic lines corresponding to either arcs of circles orthogonal to the
 187 boundary of the disk, or diameters of the disk if the line passes through the origin.
 188 The Poincaré disk intrinsically provides the look and feel of hyperbolic space
 189 in the browser. The “focus+context” mentioned before is due to the Poincaré
 190 projection. A small area near the border of the disk represents a very large
 191 area in hyperbolic space, while the same size area near the center of the disk
 192 represents a small area of hyperbolic space. This can be seen mathematically in
 193 the transformation that takes the hyperbolic plane to the Poincaré disk

$$194 \quad (r, \theta) \mapsto \left(\frac{e^r - 1}{e^r + 1}, \theta\right)$$

195 The exponentiation in the Poincaré transformation implies a practical limit
 196 on the hyperbolic radius of about 700, as larger values require dealing with very
 197 large numbers and lead to numerical overflow.

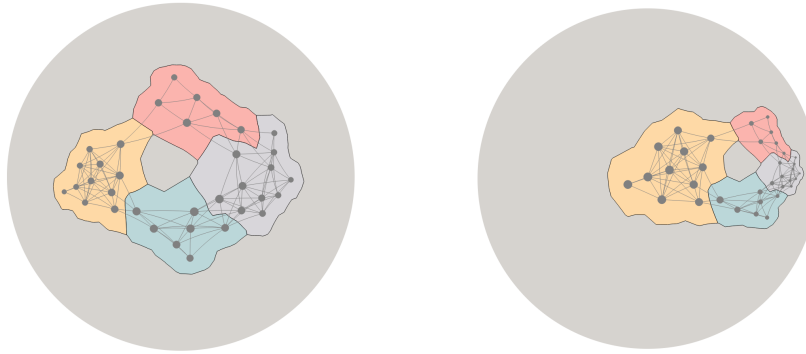
198 3.2 Interactive Features

199 **Navigating the Map:** One of the main reasons for using map-like visualization
 200 for graphs is our familiarity with map interactions such as pan, zoom, click and
 201 drag. In the Poincaré disk, clicking and dragging brings new nodes and regions
 202 into focus, allowing the viewer to exploit the “focus+context” property of the
 203 projection. We accomplish this by making use of Möbius transformations.

204 A Möbius transformation is a complex function of the form $f(z) = \frac{az+b}{cz+d}$
 205 where z is a complex variable and $ad - bc \neq 0$. Möbius transformations have
 206 many uses in complex analysis and geometry, but one subgroup is especially
 207 useful for our purposes; the class of transformations that map the open unit disk
 208 to itself. In particular the transformation

$$209 \quad f(z) = \frac{z - z_0}{-\bar{z}_0 z + 1}$$

210 takes z_0 to the origin and preserves the Poincaré projection of the hyperbolic
 211 plane, i.e., the transformation recenters the Poincaré projection at z_0 .

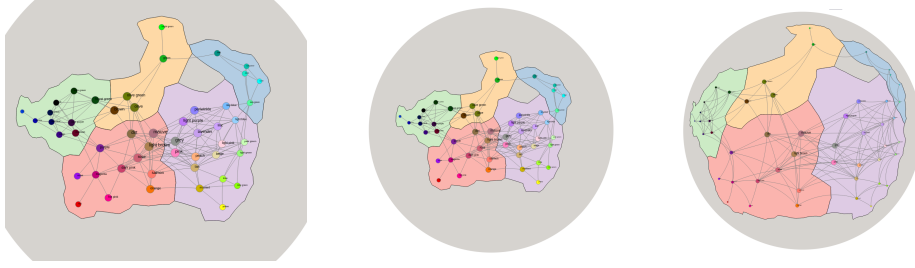


212 **Fig. 6.** The same graph centered about two different origins.

213 We can obtain transitions that look smooth to the human eye by repeatedly
 214 applying the above transformation at a point some ϵ distance from the previous
 215 origin in the direction the mouse is being dragged. Two still images centered at
 216 different points in a random graph are shown in Figure 6, but interacting with
 217 the actual visualization in GMap best conveys the idea.

220 **Zoom and Coverage:** We define two different notions of scale on the Poincaré
 221 disk that a viewer can adjust via sliders. The notion of zooming is fairly straight-
 222 forward and controls the size of the Poincaré disk in the browser window. In-
 223 tuitively, the zoom slider brings the disk closer or further away from the point
 224 of perspective; see Fig 7. Coverage controls the total area the layout occupies,
 225 which poses interesting challenges. As a consequence of Euclid’s parallel pos-
 226 tulate not holding in hyperbolic space, the hyperbolic plane is not invariant to
 227 scale [35]. However, we can re-scale the layout while it is still in the Euclidean
 228 plane, before we project it to H^2 . We do just that and by default we use a scal-
 229 ing factor of 0.005, which works well for the layouts that GMap generates. The
 230 coverage slider allows us to change the size of the layout in the Poincaré disk.

231 Lamping *et al.* [23] proposed to adjust the radial component using a non-
 232 conformal mapping that increases the distance an object was from the center



218 **Fig. 7.** An example of the default layout (center), increased zoom (left), and
 219 increased coverage (right).

233 of the disk. This method is not well-suited for our purposes, however, as it
 234 increases detail near the center of the layout, but distorts shapes further away.
 235 We instead exploit the friendly properties of the Euclidean plane, by projecting
 236 the layout back to the Euclidean plane (using the hyperbolic Lambert azimuthal
 237 projection), applying the desired scale factor, and then re-projecting it (using
 238 the inverse of the same projection).

239 **Reset, Recenter, Labels and Opacity:** While a viewer need not be an expert
 240 in hyperbolic geometry to use the visualization we provide, some properties of
 241 the geometry call for additional features to make the system more useful.

242 Given the infinite space and “focus+context” nature of the Poincaré projec-
 243 tion, it is not unreasonable that a viewer may lose sight of the layout or even
 244 become unsure of “where” they are. To alleviate this potential problem, we pro-
 245 vide a *reset button*, that brings us back to the original view. A viewer can also
 246 double-click on a node/region to *recenter* the projection at that point.

247 The number of edges near the border in large node-link diagrams and maps
 248 might increase to a level where the layout is difficult to discern. An edge *opacity*
 249 *slider* helps mitigate this problem. A related problem is that labels near the
 250 border can start to overlap. Although label size scales with distance from the
 251 origin, the two scales are necessarily different (as distances can approach infinity
 252 and label sizes cannot). To help remedy this, we provide a *label size slider*, which
 253 adjusts the relative label sizes on the fly.

254 3.3 Considerations

255 The inherent distortion of shapes and angles introduced when using the inverse
 256 Lambert projection to the hyperbolic plane implies that at some threshold the
 257 outer regions of the layout will become too distorted to be of use. This is already
 258 apparent in the MusicLand example from GMap as shown in Figure 8, with
 259 around 250 nodes. Even though our method can handle larger graphs, it is clear
 260 that larger graphs pose additional challenges. A multi-level representation of the
 261 graph might be useful to provide “semantic zooming” where we start with a high

level overview of the graph and zooming in brings up more details, following
 Schneiderman’s mantra (overview first, zoom and filter, details on demand).
 Different inverse hyperbolic projections might also be useful and worth exploring.

When moving through a curved space, an inherent property causes an ob-
 server to incur rotation. This could be desirable, as it gives several different
 perspectives on the same layout, but it could potentially be confusing when nav-
 igating large maps. Specifically, moving the layout in the Poincaré disk, incurs
 a rotation in the layout (clockwise or counter-clockwise): consider translating a
 layout some fixed distance up, the same distance to the right, then again down,
 and back to the left. In 2D Euclidean geometry, the layout would be identical
 after these transformations. However, in the Poincaré disk (and hyperbolic ge-
 ometry in general) this will cause the layout to be rotated about 90 degrees
 from its original orientation. An orientation correcting transformation could be
 applied after translating the layout, but in our prototype we only provide the
 “reset button,” which resets the original layout.

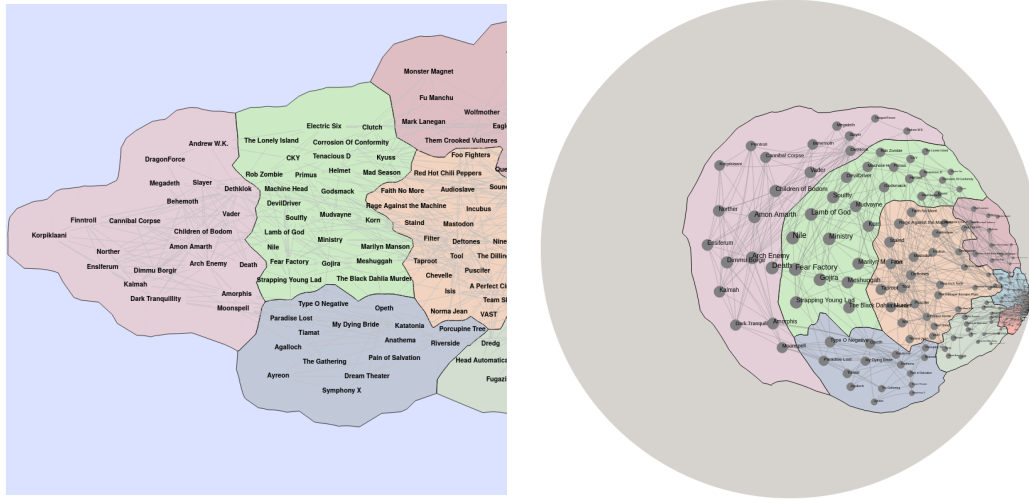


Fig. 8. A 2D Euclidean GMap instance of the MusicLand graph (left) and its
 hyperbolic realization (right).

4 Force-directed Method

Our projection-based hyperbolic visualization method uses a precomputed 2-
 dimensional Euclidean layout, but it uses hyperbolic space just for the visual-
 ization and “focus+context” effect, rather than for the actual graph embedding.
 Properly embedding the graph in hyperbolic space would allow us to take advan-
 tage of the underlying hyperbolic geometry. Algorithms for directly embedding

285 special classes of graphs in hyperbolic space, such as trees and hierarchies, can
 286 better take advantage of the properties of the space and obtain better embed-
 287 dings than via projections. It is also possible to modify the standard force-
 288 directed algorithm for operation in Riemannian geometries (such as hyperbolic
 289 and spherical) by taking advantage of the locally Euclidean properties of such
 290 spaces [20]. The implementation, which provides visualization in the browser,
 291 can be found at <https://github.com/Mickey253/hyperbolic-space-graphs>.

292 The idea is to compute a tangent plane at each vertex embedded in the
 293 non-Euclidean Riemannian space, mapping every other vertex to that plane,
 294 performing a step of a force-directed algorithm in the plane, and projecting
 295 back the resulting node position changes to the Riemannian space. While con-
 296 ceptually simple, this method allows the graph to make use of the unique prop-
 297 erties of the corresponding non-Euclidean geometry. For instance, on the sphere,
 298 3-dimensional polytopes wrap “around” the sphere, more accurately realizing
 299 their structure than anything that can be done in the plane [32].

300 We apply this idea to the Kamada-Kawai type of force-directed graph layout
 301 algorithm, for its conceptual simplicity and its desirable property of capturing
 302 graph structure (e.g., graph distances between pairs of nodes) in the embedding
 303 (e.g., realized distances between pairs of nodes in the non-Euclidean space).
 304 Specifically, we compute the graph theoretic distances between all pairs of nodes
 305 and these define desired distances in the layout. Spring forces, proportional to the
 306 squared Euclidean distance between nodes in the layout, are used to gradually
 307 improve a given initial layout to one in which realized distances match the graph
 308 theoretic distances [18]. Formally, there is an attractive or repulsive force (similar
 309 to stress) defined for any pair of edges based on the difference between the
 310 graph theoretical distance and the realized distance in the current embedding.
 311 Specifically, the total energy of the system is modeled as:

$$312 \quad E = \sum_{i=1}^{n-1} \sum_{j=i+1}^n \frac{1}{2} k_{ij} (|p_i - p_j| - d_{ij})^2$$

313 where given a pair of nodes i and j d_{ij} is the graph theoretic distance between
 314 them, $|p_i - p_j|$ is the current realized distance in the embedding between them,
 315 and k_{ij} is the strength of the spring forces between them. The layout is obtained
 316 by reducing the energy of the system via gradient descent.

318 4.1 Tangent plane

319 In order to compute a tangent plane at some point x in H^2 , we need to set the
 320 distance between x and every other point in the plane to the hyperbolic distance
 321 between them, and ensure the angle between the points stays the same [20]. The
 322 Poincaré disk preserves angles, so we only need to map hyperbolic to Euclidean
 323 distances. In the Poincaré model, hyperbolic distance is simplest to compute
 324 when one point is at the origin, so we first apply the Möbius transformation

pronounced on the Poincaré disk, as the number of bits needed to accurately reflect the hyperbolic position increases exponentially as one approaches the border of the disk. We choose to trade accuracy for stability: if a node is pushed to a within 0.001 of the border, then the node is “pulled back” so it does not disappear altogether. This effectively creates a bounding region defined by a circle of (Euclidean) radius 0.999 from the center of the Poincaré disk.

4.3 Considerations

Unlike the sphere where there are natural graphs that can be realized on the sphere but not the plane (e.g., 3-dimensional polytopes), it is not clear what are simple examples that illustrate that our method is in fact making good use of the hyperbolic geometry. A path does converge to a geodesic in our implementation, so this is a good indication. Trees span out evenly as one might expect in hyperbolic space, and several other layouts are shown in Appendix A.

Currently our hyperbolic force directed approach only works for node-link diagrams. Extending its utility to map-like visualizations (such as GMap, BubbleSets, MapSets, LineSets) could be accomplished by projecting the completed layout of the graph onto the plane, computing the needed clusters and polygons, then projecting them back onto the Poincaré disk. Better yet, we could perform the clustering and polygon-generation directly in hyperbolic space. The cluster regions (polygons) are computed using Voronoi diagrams in GMap and it has been shown that Voronoi diagrams for 2-dimensional points generalize to hyperbolic space and can be computed in $O(n \log n)$ time [30].

5 Discussion, Conclusions and Future Work

We described two methods for visualizing graphs in hyperbolic space. The projection-based method is fully functional at <http://gmap.cs.arizona.edu> and provides all the layout algorithms, clustering algorithms and visualization styles available within GMap. The projection-based method allows us to show any 2-dimensional Euclidean visualization in hyperbolic space, where we can take advantage of the “focus+context” properties of the space while still relying on standard map interactions. The method currently relies on Lambert azimuthal projections and the Poincaré disk model. We have not yet explored other projections or the Beltrami-Klein model. Finally, this method does not fully take advantage of the underlying geometry of the space.

The force-directed method uses the non-Euclidean geometry better and is also fully functional at <https://github.com/Mickey253/hyperbolic-space-graphs>. This method does utilize the geometry of hyperbolic space, but is not as efficient as the projection-based one. The underlying Kamada-Kawai algorithm is already rather computationally expensive with a pre-processing of an all-pairs shortest path (implemented with an $O(|V|^3)$ algorithm, where $|V|$ is the number of nodes in the graph) and the many tangent plane computations are also time-consuming. It can take nearly one minute to compute a layout for graph with 100 nodes,

and the running time becomes prohibitively expensive for larger graphs. We have not yet implemented scalable force-directed algorithms, or a multi-level ones, and this is a natural direction for future work.

While there is good evidence for the potential advantage of visualizing graphs in non-Euclidean spaces, we are not aware of human-subjects studies evaluating the effectiveness of such of non-Euclidean graph visualization. Now that GMap conveniently includes Euclidean layouts as well as spherical and hyperbolic realizations this may be something to consider. We have not performed quantitative evaluations either, besides measuring runtimes and there are several adjustable parameters that can and should be optimized.

We have also not yet evaluated whether graphs that are supposed to be better embeddable in hyperbolic space [7], do indeed realize their underlying structure better in hyperbolic than in Euclidean space. Virtual reality and augmented reality provide promising applications for hyperbolic visualization, although prior work seems to have only considered spherical space in this context [22]. Finally, we want to compute a graph layout directly in hyperbolic space (not relying on the Euclidean plane at all) which requires generalizations to non-Euclidean geometry of Euclidean techniques such as MDS [36], t-SNE [24] and UMAP [25].

References

1. Alper, B., Riche, N.H., Ramos, G.A., Czerwinski, M.: Design study of LineSets, a novel set visualization technique. *IEEE Trans. Vis. Comput. Graph.* **17**(12), 2259–2267 (2011). <https://doi.org/10.1109/TVCG.2011.186>
2. Andrews, K., Putz, W., Nussbaumer, A.: The hierarchical visualisation system (HVS). In: 11th International Conference on Information Visualisation, IV 2007, 2-6 July 2007, Zürich, Switzerland. pp. 257–262. IEEE Computer Society (2007). <https://doi.org/10.1109/IV.2007.112>
3. Barry, N.: Hyperbolic Canvas Github Page. <https://github.com/ItsNickBarry/hyperbolic-canvas>, accessed: 2021-06-06
4. Baumgartner, J., Waugh, T.A.: Roget2000: a 2d hyperbolic tree visualization of Roget’s thesaurus. In: Erbacher, R.F., Chen, P.C., Gröhn, M., Roberts, J.C., Wittenbrink, C.M. (eds.) *Visualization and Data Analysis 2002*, San Jose, CA, USA, January 19, 2002. SPIE Proceedings, vol. 4665, pp. 339–346. SPIE (2002). <https://doi.org/10.1117/12.458803>
5. Belmonte, N.G.: Javascript InfoVis Toolkit. <https://philogb.github.io/jit/demos.html>, accessed: 2021-06-06
6. Bingham, J., Sudarsanam, S.: Visualizing large hierarchical clusters in hyperbolic space. *Bioinform.* **16**(7), 660–661 (2000). <https://doi.org/10.1093/bioinformatics/16.7.660>
7. Bläsius, T., Friedrich, T., Krohmer, A., Laue, S.: Efficient embedding of scale-free graphs in the hyperbolic plane. *IEEE/ACM Trans. Netw.* **26**(2), 920–933 (2018). <https://doi.org/10.1109/TNET.2018.2810186>
8. Bou, B.: Treebolic2 Webpage. <http://treebolic.sourceforge.net/treebolic2/en/index.html>, accessed: 2021-06-06
9. Celinska, D., Kopczynski, E.: Programming languages in GitHub: A visualization in hyperbolic plane. In: *Proceedings of the Eleventh International Conference on Web*

- 428 and Social Media, ICWSM 2017, Montréal, Québec, Canada, May 15-18, 2017. pp.
429 727–728. AAAI Press (2017), [https://aaai.org/ocs/index.php/ICWSM/ICWSM17/
430 paper/view/15583](https://aaai.org/ocs/index.php/ICWSM/ICWSM17/paper/view/15583)
- 431 10. Collins, C., Penn, G., Carpendale, S.: BubbleSets: Revealing set relations with
432 isocontours over existing visualizations. *IEEE Trans. Vis. Comput. Graph.* **15**(6),
433 1009–1016 (2009). <https://doi.org/10.1109/TVCG.2009.122>
- 434 11. Efrat, A., Hu, Y., Kobourov, S., Pupyrev, S.: MapSets: Visualizing embed-
435 ded and clustered graphs. *J. Graph Algorithms Appl.* **19**(2), 571–593 (2015).
436 <https://doi.org/10.7155/jgaa.00364>
- 437 12. Gansner, E.R., Hu, Y., Kobourov, S.: GMap: Visualizing graphs and clus-
438 ters as maps. In: *IEEE Pacific Visualization Symposium PacificVis 2010*,
439 Taipei, Taiwan, March 2-5, 2010. pp. 201–208. IEEE Computer Society (2010).
440 <https://doi.org/10.1109/PACIFICVIS.2010.5429590>
- 441 13. Glatzhofer, M.: Hyperbolic tree of life. [https://hyperbolic-tree-of-life.
442 github.io/](https://hyperbolic-tree-of-life.github.io/), accessed: 2021-06-06
- 443 14. Glatzhofer, M.: Hyperbolic Browsing. Master’s thesis, Institute of Interactive Sys-
444 tems and Data Science (ISDS),Graz University of Technology, Austria (2018)
- 445 15. Glatzhofer, M.: d3-hypertree Github page. [https://github.com/glouwa/
446 d3-hypertree](https://github.com/glouwa/d3-hypertree), accessed: 2021-06-06
- 447 16. Hu, Y.: Efficient, high-quality force-directed graph drawing. *Mathematica journal*
448 **10**(1), 37–71 (2005)
- 449 17. Hyun, Y.: <https://www.caida.org/catalog/software/walrus/#H2540> (2000),
450 accessed: 2021-06-06
- 451 18. Kamada, T., Kawai, S.: An algorithm for drawing general undirected graphs. *Inf.*
452 *Process. Lett.* **31**(1), 7–15 (1989). [https://doi.org/10.1016/0020-0190\(89\)90102-6](https://doi.org/10.1016/0020-0190(89)90102-6)
- 453 19. Kobourov, S.: Spring embedders and force directed graph drawing algorithms.
454 *CoRR abs/1201.3011* (2012), <http://arxiv.org/abs/1201.3011>
- 455 20. Kobourov, S., Wampler, K.: Non-Euclidean spring embedders. *IEEE Trans. Vis.*
456 *Comput. Graph.* **11**(6), 757–767 (2005). <https://doi.org/10.1109/TVCG.2005.103>
- 457 21. Krioukov, D.V., Papadopoulos, F., Kitsak, M., Vahdat, A., Boguñá, M.: Hy-
458 perbolic geometry of complex networks. *CoRR abs/1006.5169* (2010), [http:
459 //arxiv.org/abs/1006.5169](http://arxiv.org/abs/1006.5169)
- 460 22. Kwon, O., Muelder, C., Lee, K., Ma, K.: A study of layout, rendering, and interac-
461 tion methods for immersive graph visualization. *IEEE Trans. Vis. Comput. Graph.*
462 **22**(7), 1802–1815 (2016). <https://doi.org/10.1109/TVCG.2016.2520921>
- 463 23. Lamping, J., Rao, R., Pirolli, P.: A focus+context technique based on hyperbolic
464 geometry for visualizing large hierarchies. In: Katz, I.R., Mack, R.L., Marks, L.,
465 Rosson, M.B., Nielsen, J. (eds.) *Human Factors in Computing Systems, CHI ’95*
466 *Conference Proceedings*, Denver, Colorado, USA, May 7-11, 1995. pp. 401–408.
467 ACM/Addison-Wesley (1995). <https://doi.org/10.1145/223904.223956>
- 468 24. Van der Maaten, L., Hinton, G.: Visualizing data using t-sne. *Journal of machine*
469 *learning research* **9**(11) (2008)
- 470 25. McInnes, L., Healy, J.: UMAP: uniform manifold approximation and projection
471 for dimension reduction. *CoRR abs/1802.03426* (2018), [http://arxiv.org/abs/
472 1802.03426](http://arxiv.org/abs/1802.03426)
- 473 26. Munzner, T.: H3: laying out large directed graphs in 3d hyperbolic space.
474 In: *1997 IEEE Symposium on Information Visualization (InfoVis ’97)*, Octo-
475 ber 18-25, 1997, Phoenix, AZ, USA. pp. 2–10. IEEE Computer Society (1997).
476 <https://doi.org/10.1109/INFVIS.1997.636718>

- 477 27. Munzner, T.: Exploring large graphs in 3d hyperbolic space.
 478 IEEE Computer Graphics and Applications **18**(4), 18–23 (1998).
 479 <https://doi.org/10.1109/38.689657>, <https://doi.org/10.1109/38.689657>
- 480 28. Munzner, T.: Interactive visualization of large graphs and networks. Ph.D. thesis,
 481 Stanford University (2000)
- 482 29. Munzner, T., Burchard, P.: Visualizing the structure of the world wide web
 483 in 3d hyperbolic space. In: Nadeau, D.R., Moreland, J.L. (eds.) *Proced-*
 484 *ings of the 1995 Symposium on Virtual Reality Modeling Language, VRML*
 485 *1995*, San Diego, CA, USA, December 14–15, 1995. pp. 33–38. ACM (1995).
 486 <https://doi.org/10.1145/217306.217311>
- 487 30. Nielsen, F., Nock, R.: Hyperbolic voronoi diagrams made easy. In: Apduhan, B.O.,
 488 Gervasi, O., Iglesias, A., Taniar, D., Gavrilova, M.L. (eds.) *Prodeedings of the 2010*
 489 *International Conference on Computational Science and Its Applications, ICCSA*
 490 *2010*, Fukuoka, Japan, March 23–26, 2010. pp. 74–80. IEEE Computer Society
 491 (2010). <https://doi.org/10.1109/ICCSA.2010.37>
- 492 31. Ontrup, J., Ritter, H.J.: Hyperbolic self-organizing maps for semantic navigation.
 493 In: Dietterich, T.G., Becker, S., Ghahramani, Z. (eds.) *Advances in Neural In-*
 494 *formation Processing Systems 14* [*Neural Information Processing Systems: Natu-*
 495 *ral and Synthetic, NIPS 2001, December 3–8, 2001, Vancouver, British Columbia,*
 496 *Canada*]. pp. 1417–1424. MIT Press (2001), [https://proceedings.neurips.cc/](https://proceedings.neurips.cc/paper/2001/hash/093b60fd0557804c8ba0cbf1453da22f-Abstract.html)
 497 [paper/2001/hash/093b60fd0557804c8ba0cbf1453da22f-Abstract.html](https://proceedings.neurips.cc/paper/2001/hash/093b60fd0557804c8ba0cbf1453da22f-Abstract.html)
- 498 32. Perry, S., Yin, M.S., Gray, K., Kobourov, S.: Drawing graphs on the sphere. In:
 499 Tortora, G., Vitiello, G., Winckler, M. (eds.) *AVI '20: International Conference*
 500 *on Advanced Visual Interfaces*, Island of Ischia, Italy, September 28 - October 2,
 501 2020. pp. 17:1–17:9. ACM (2020). <https://doi.org/10.1145/3399715.3399915>
- 502 33. Saket, B., Scheidegger, C., Kobourov, S., Börner, K.: Map-based visualizations
 503 increase recall accuracy of data. *Comput. Graph. Forum* **34**(3), 441–450 (2015).
 504 <https://doi.org/10.1111/cgf.12656>
- 505 34. Saket, B., Simonetto, P., Kobourov, S., Börner, K.: Node, node-link, and node-
 506 link-group diagrams: An evaluation. *IEEE Trans. Vis. Comput. Graph.* **20**(12),
 507 2231–2240 (2014). <https://doi.org/10.1109/TVCG.2014.2346422>
- 508 35. Sala, F., Sa, C.D., Gu, A., Ré, C.: Representation tradeoffs for hyperbolic embed-
 509 dings. In: Dy, J.G., Krause, A. (eds.) *Proceedings of the 35th International Confer-*
 510 *ence on Machine Learning, ICML 2018, Stockholmsmässan, Stockholm, Sweden,*
 511 *July 10–15, 2018. Proceedings of Machine Learning Research*, vol. 80, pp. 4457–
 512 4466. PMLR (2018), <http://proceedings.mlr.press/v80/sala18a.html>
- 513 36. Shepard, R.N.: The analysis of proximities: multidimensional scaling with an un-
 514 known distance function. i. *Psychometrika* **27**(2), 125–140 (1962)
- 515 37. Snyder, J.P.: *Map projections: A working manual*. U.S. Government Printing Office
 516 (1987). <https://doi.org/10.3133/pp1395>
- 517 38. Walter, J.A., Ritter, H.J.: On interactive visualization of high-dimensional
 518 data using the hyperbolic plane. In: *Proceedings of the Eighth ACM*
 519 *SIGKDD International Conference on Knowledge Discovery and Data Min-*
 520 *ing*, July 23–26, 2002, Edmonton, Alberta, Canada. pp. 123–132. ACM (2002).
 521 <https://doi.org/10.1145/775047.775065>
- 522 39. Zhang, S., Kelleher, A.: H3py Github Page. <https://github.com/buzzfeed/pyh3>
 523 (2016), accessed: 2021-06-06

6 Appendix A: Generated Layouts

Appendix A includes further examples of layouts generated by our force-directed layout approach that did not fit into the body of the paper. The captions of each image briefly describe the graph and parameters. The source code that generated can be found at <https://github.com/Mickey253/hyperbolic-space-graphs>, along with links to videos showcasing the algorithm in action.

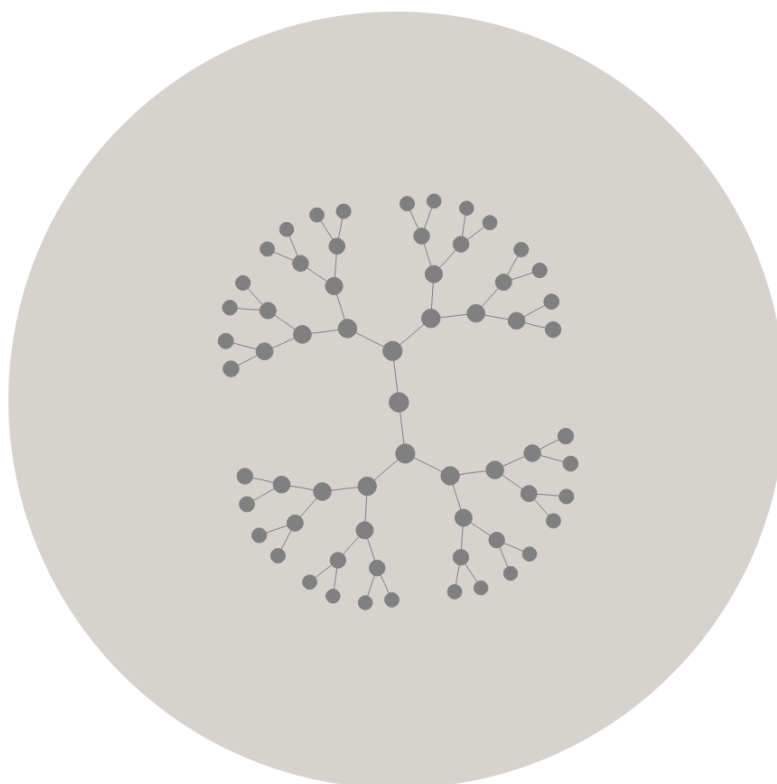


Fig. 10. A 63 node binary tree with edge length 2.

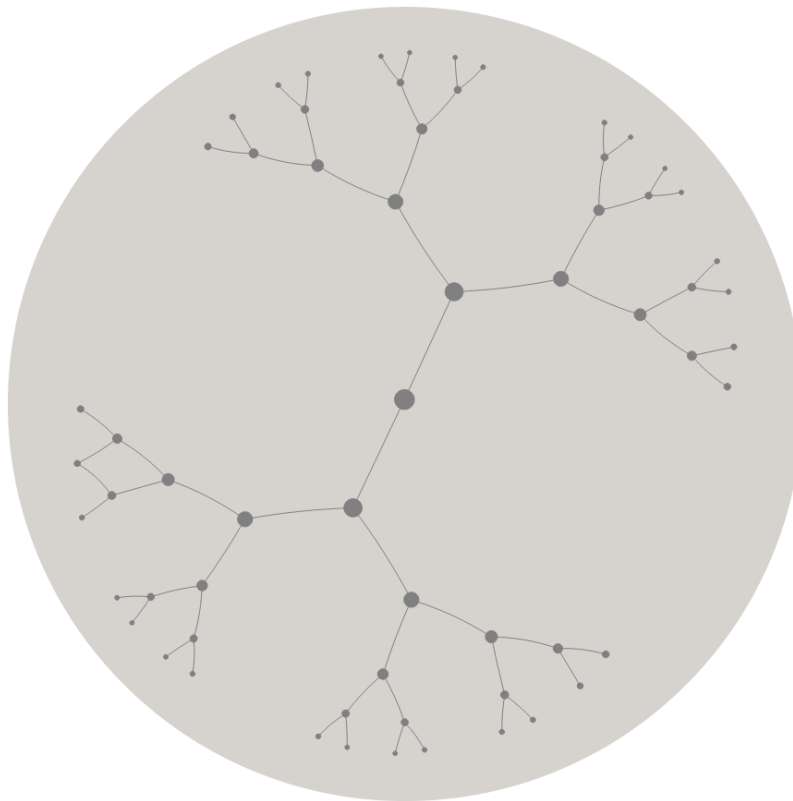


Fig. 11. A 63 node binary tree with edge length 5.

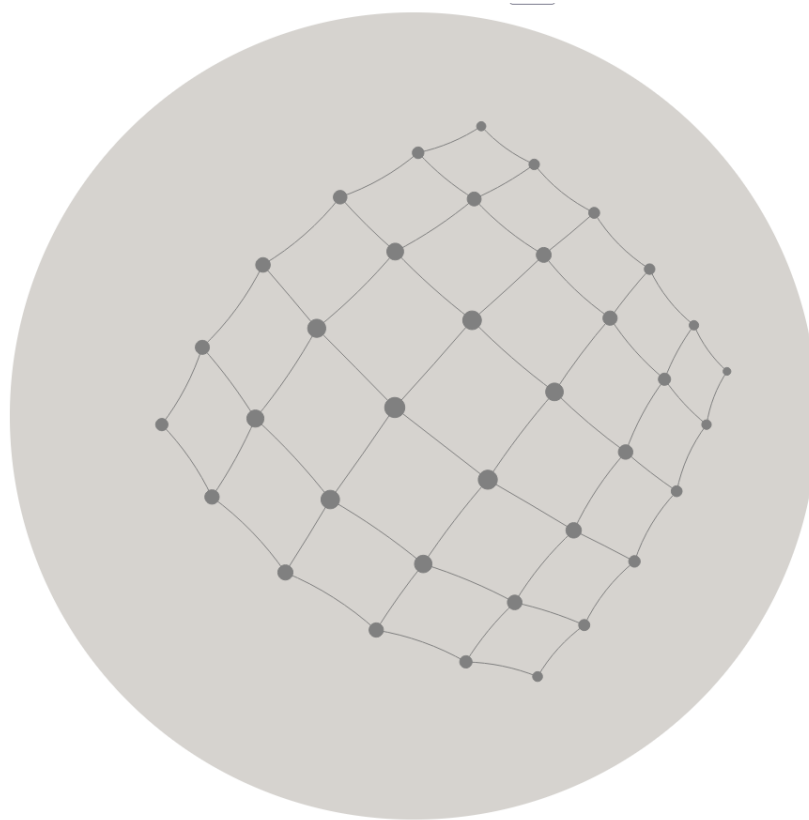


Fig. 12. A 6x6 grid graph with ideal edge length 5.

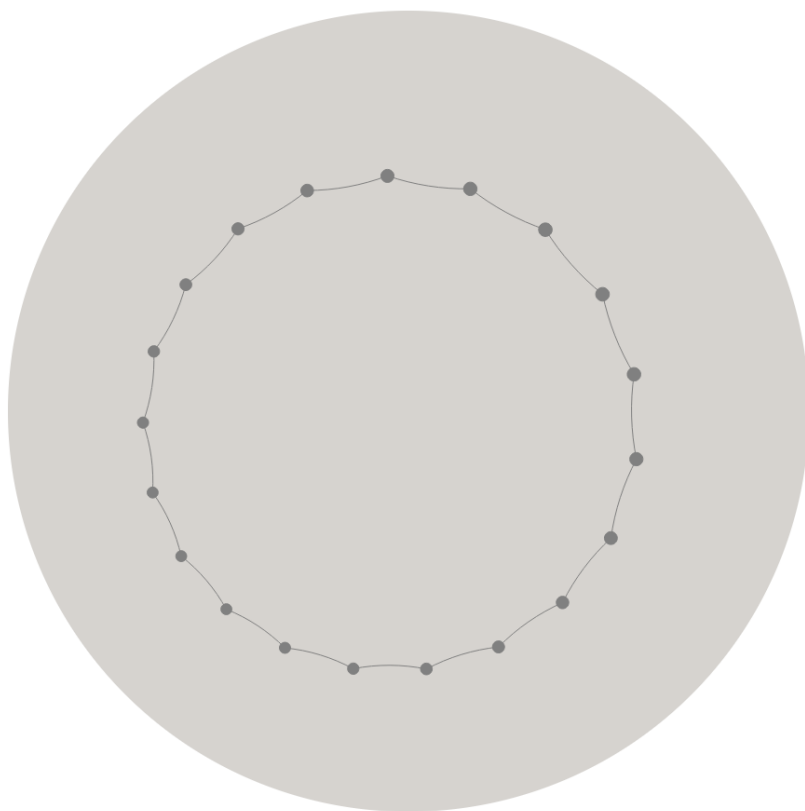


Fig. 13. A ring graph.

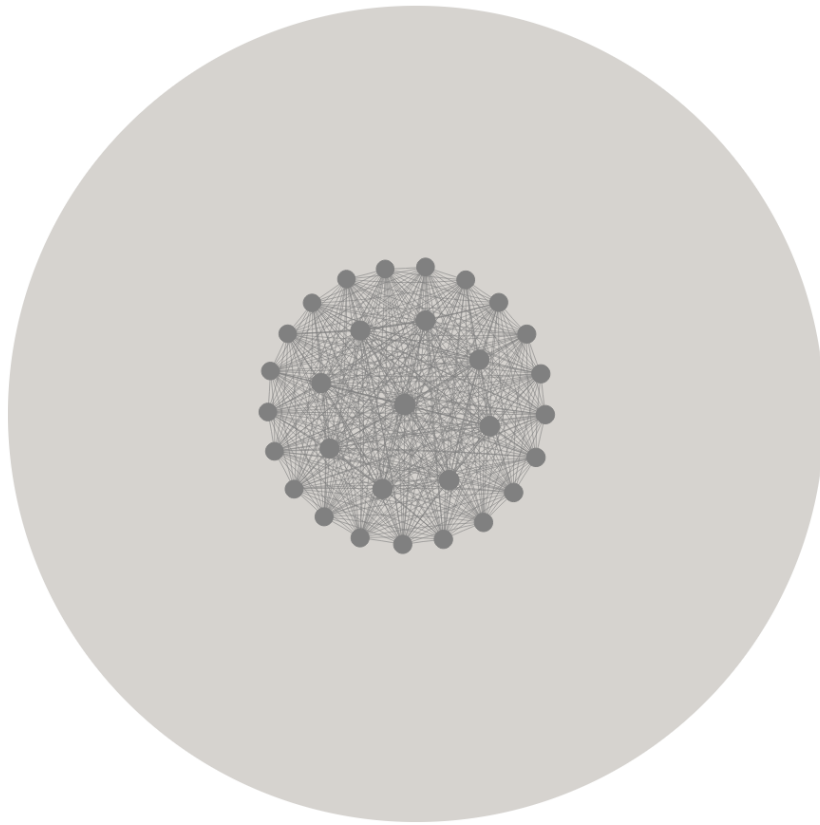


Fig. 14. A complete graph on 30 nodes.

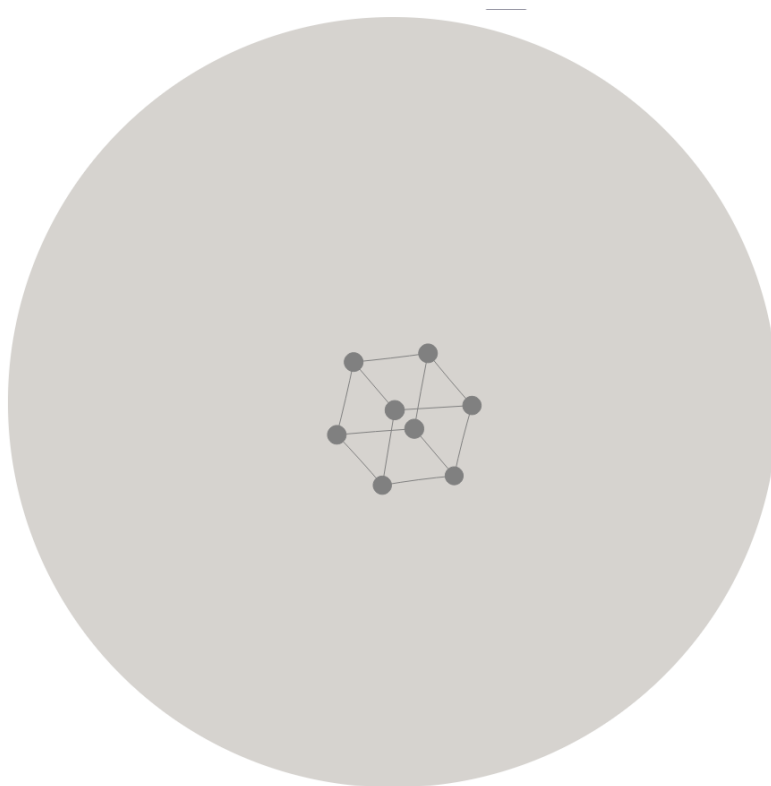


Fig. 15. A cube with an ideal edge length of 1.

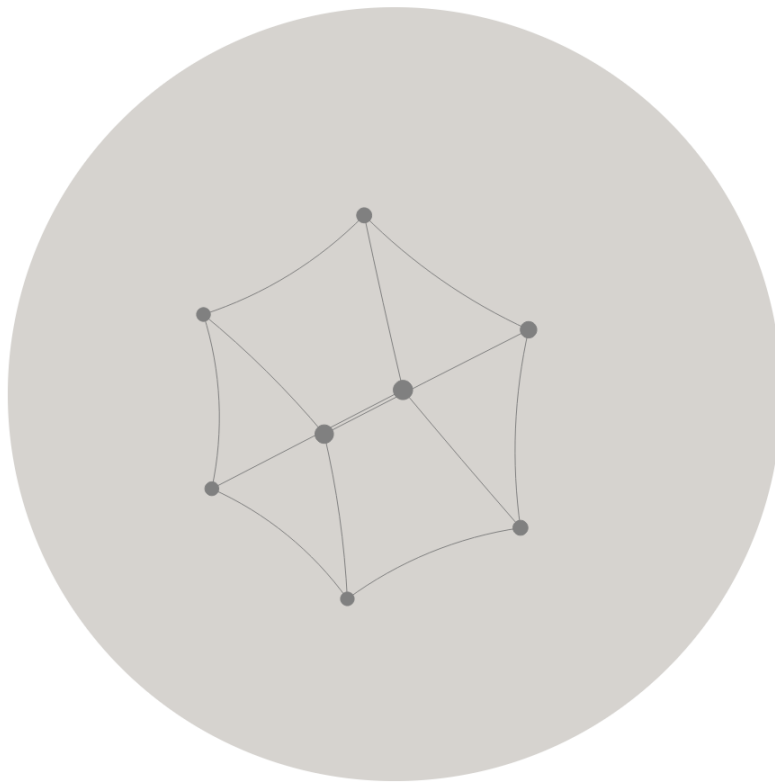


Fig. 16. A cube with an ideal edge length of 3.



Fig. 17. A dodecahedron.